

Parametric Study of Concrete Dam Stability By Using Abaqus Software

Thamir Mohammed Ahmed ^{1*}  and Abdullah Hassan Azbah ¹ 

¹ Civil Engineering Department, Engineering Faculty, Tishk International University, Erbil-Iraq

Article History

Received: 08.07.2023

Revised: 14.11.2023

Accepted: 23.11.2023

Published: 08.01.2024

Communicated by: Dr. Orhan Tug

*Email address:

thamir.ahmed@tiu.edu.iq

*Corresponding Author



Copyright: © 2023 by the author.

Licensee Tishk International University, Erbil, Iraq. This article is an open access article distributed under the terms and conditions of the

Creative Commons Attribution-NonCommercial 2.0 Generic License (CC BY-NC 2.0)

<https://creativecommons.org/licenses/by-nc/2.0/>

Abstract:

This study analyzes a concrete dam using Abaqus software at different water storage levels (60m, 70m, and 80m). The dam sections are designed based on these levels using approved equations by the United States Bureau of Reclamation. Static and dynamic forces, including seismic components, are calculated for worst-case scenarios. The analysis considers cases with and without galleries, varying the dam base width. Stresses (vertical, shear, and main) are calculated and presented as curves for comparison. The study examines the impact of reservoir water levels, additional base parts, and galleries on dam stability. Findings show that galleries significantly affect stress distribution, causing stress concentrations near openings. Normal stress is uniform except at the gallery, where it decreases. Maximum water storage leads to slight increases in normal stress. Without a gallery, normal stress increases until a certain distance, then decreases towards the pre-toe region, with maximum stress at the toe. The length of the additional base has a limited effect on normal stress. The presence of a gallery affects principal stress distribution, with higher values near the toe region for higher storage levels. The shear stress distribution is more uniform without a gallery. These findings demonstrate the complex interaction of factors in concrete dam stress behavior. Proper consideration of these factors is crucial for design, analysis, and maintenance to ensure structural integrity and performance. Further analysis considering material properties, loading conditions, and dam geometry would enhance understanding and facilitate precise design and safety assessments.

Keywords: Concrete Dams; Stability; Additional Parts; Gallery; Normal Stress; Shear Stress; Principal Stress.

1. Introduction

Concrete dams serve as vital infrastructure with multifaceted benefits, including flood control, hydroelectric power generation, and water supply. Ensuring the longevity and effectiveness of these structures requires a comprehensive understanding of their behavior. Many previous studies emphasize the necessity of rigorous analysis methods, including physical testing, analytical modeling, and numerical simulation. The increasing importance of concrete dam design and construction is highlighted, especially in the context of factors affecting dam performance.

Many previous studies contributed distinct perspectives to the obvious understanding of concrete dam dynamics. Hamdi and Al-Shadidi's (2017) research delves into the structural stability of small concrete gravity dams, optimizing sections to balance cost-effectiveness and safety. Zhu, Gu, Qiu, and Li (2016) focus on assessing seepage safety under heavy rainfall and short-duration storms, using advanced statistical models and a quantum genetic algorithm. The evolution of dam safety assessment methodologies, as highlighted has been discussed by Segura, Mikkell, Poulter, and Padgett (2021). This study presents a probability-based approach, offering a robust and computationally efficient alternative to traditional methods. It emphasizes the challenges posed by existing dams that do not meet updated standards and the cost of achieving compliance through structural rehabilitation.

The importance of laboratory tests in simulating hydrodynamic loads is discussed, in previous work by Gbara and Jimianz (1998). Mostly, the studies emphasize the importance of stability standards established by reputable organizations such as the U.S. Bureau of Reclamation (USBR) and the U.S. Army Corps of Engineers in ensuring the safe operation of dams. It presents seismic considerations and highlights the necessity of mathematical models to evaluate the effect of seismic forces on dam stability.

The specific parameters that affect dam stability, such as normal vertical stress, coefficient of friction, and footing width, have been studied by Ahmed (2016), Arnab et al. (2015), Elias et al. (2014) are incorporated into the narrative, presenting their contributions to understanding the effects of increasing the dam base, introducing the OPTIDAM program, and investigating critical parameters affecting concrete gravity dams.

In this study, the focus extends to the design and analysis of different sections of the concrete dam, including the gallery, and considering different water levels. This research aims to identify the main factors affecting the safety of dams and to contribute to a broader body of knowledge on the stability of concrete dams. Thus, the results weave together diverse studies to enrich the data and information regarding concrete dam stability.

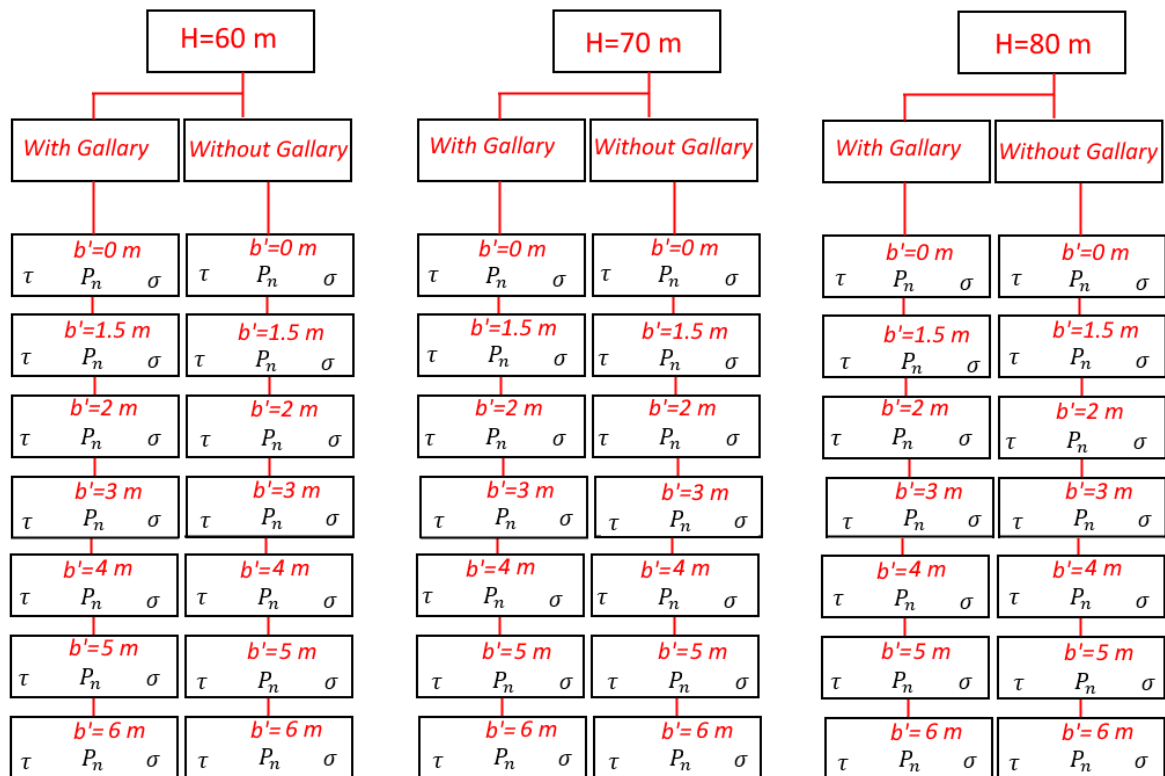
2. Methodology

In this study, a comprehensive analysis of the concrete dam was performed using Abaqus software, which includes a set of important parameters and load scenarios. The investigation examined three different storage levels in the dam: 60 m, 70 m, and 80 m. The dam sections were designed entirely based on these varying levels, using well-established equations approved by the U.S. Bureau of Reclamation (USBR). The main properties of concrete taken into consideration are a density of 2400 kg/m³, Young's modulus of 20,000,000 N/m², and a Poisson's ratio of 0.2. The 2D Abaqus software was used for the analysis, which was performed separately for each water level (H), representing the scenarios with and without galleries. To ensure a thorough exploration of design variations, the width of the dam base was systematically varied in increments of 0, 1, 1.5, 2, 3, 4, 5, and 6 m. This careful approach aims to capture the effect of additional parts to width b' on the structural response of the dam. All static and dynamic forces acting on the dam body were calculated, focusing on the worst-case scenario of seismic force components. This included assessing the vertical forces directed upward ($0.05 W$) and horizontal forces directed downstream (D/S) of the dam ($0.1 W$), where W , is the dam weight.

These steps include a thorough calculation of the maximum and minimum principal stresses for each case studied. To enhance clarity and facilitate overall implementation, results are presented in the form of detailed curves, allowing for careful analysis and meaningful comparison of diverse scenarios. The following sections will include a detailed presentation of the factors used in reproducing the dam for each case. In addition, figures depicting the dam under different loads will be distinctively displayed, providing a visual representation to complete the engagement. This improvement aims to provide a more transparent and informative picture of the methodology used in this study.

3. Results and Discussion

In the current study, the Abaqus software is used to analyze the selected most common sections of concrete dams. The study cases included testing the effects of different values of reservoir water levels and additional base parts on the stability of dams. The study has also been focused on the effects of gallery existence, such that, the estimation of stresses is classified for with and without gallery. The cases are shown in the following flowchart:



Where τ , P_v , and σ are shear, normal, and principal stresses, respectively.

3.1 Normal Stress, P_v (with Gallery)

Figures 1, 2, and 3 clearly show the dynamic changes in normal stress along the base of the concrete dam, considering parameters such as additional parts (b') and maximum water storage (H). Central to this analysis is the incorporation of a portico at a specific distance from the heel of the dam, introducing voids and openings within the structure. The presence of the gallery greatly affects the stress distribution, creating stress concentrations near the interfaces. This complex interaction is shaped by factors such as the geometry of the gallery, its interaction with the surrounding concrete, and loading conditions.

The figures depict a fine pattern of pressure distribution, showing uniform pressure from the heel, gradually decreasing from $X = 30$ m towards its lowest values between $X = 45$ m and 60 m. It is worth noting that the normal stresses suddenly increase to their highest values at the toe point, especially for $b'=2$ m. An increase in H results in small increases in normal stress values. The discussion then delves into a comprehensive analysis of the effects of height H and base width b' on normal stress using the results table provided.

By analyzing the effect of height (H), a positive relationship between H and natural stress was observed. Increasing H , while remaining constant b' , generally results in a higher positive normal pressure. The effect of H is more pronounced when b' is smaller, which is evident in the increase in normal pressure as b' decreases at constant $H = 60$. When studying the effect of base width b' , larger base widths tend to have lower normal stress values. This effect is noticeable when comparing results at the same height (H) but different b' values, such as $b'=0$ compared to $b'=6$. The effect of b' on normal stress is more pronounced at higher elevations (H), confirming its interaction with H in determining the stress distribution.

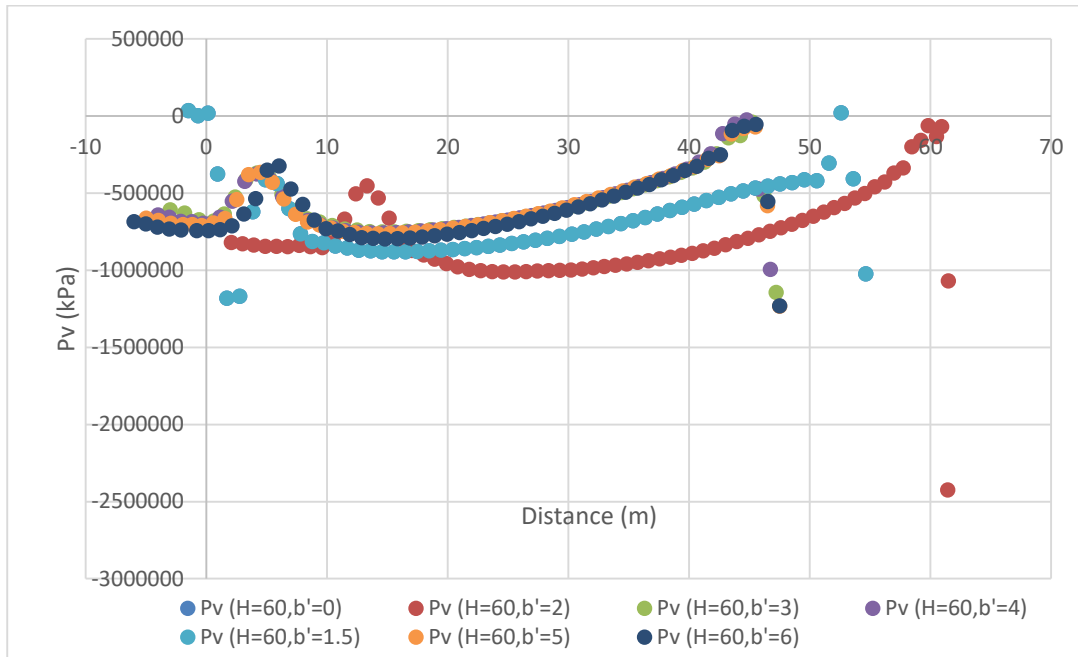


Figure 1: Variation of vertical stresses with gallery for H=60 m and different b'.

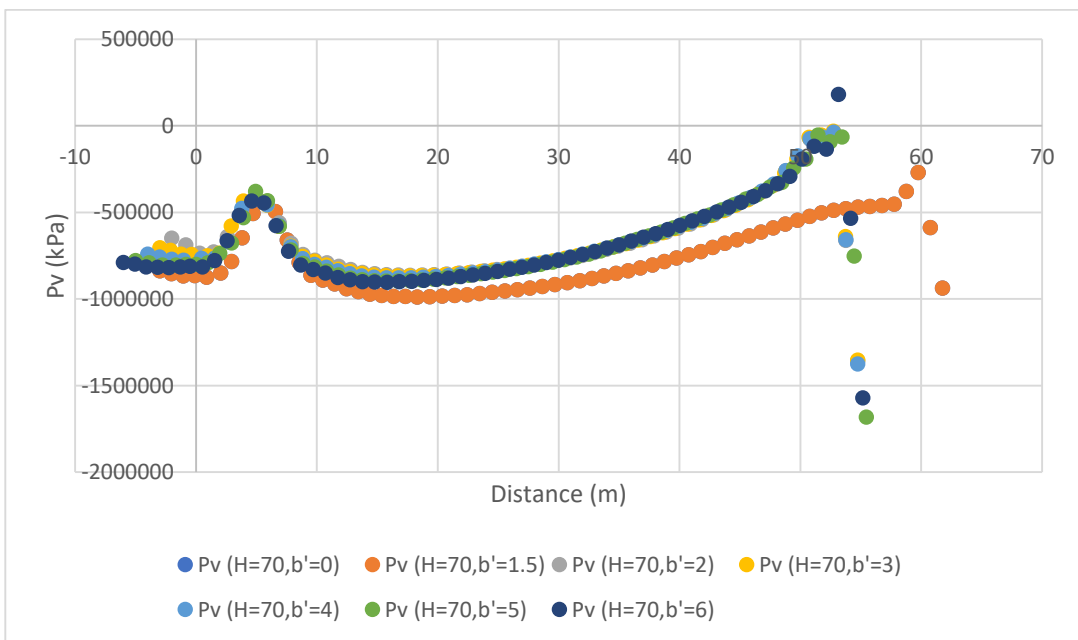


Figure 2: Variation of vertical stresses with gallery for H=70 m and different b'.

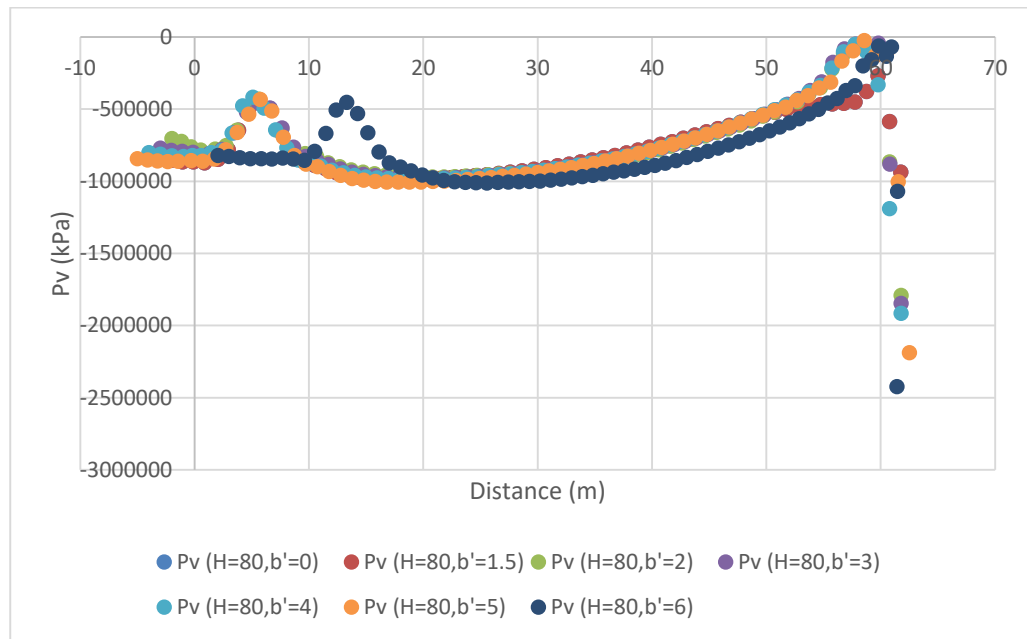


Figure 3: Variation of vertical stresses with gallery for $H=80$ m and different b' .

3.2 Normal Stress, P_v (without Gallery)

The study of the normal stresses at the base of concrete embankment sections without a colonnade, as shown in Figures 4, 5, and 6, provides insightful observations about the behavior and distribution of normal stresses. The results reveal a distinct stress profile along the base of the dam, with values increasing uniformly from low values at the heel up to $X = 20$ m. Thereafter, there is a gradual decrease until $X = 45$ m, followed by the highest instantaneously observed stress values at the toe point. The additional section length has a limited effect on the stress behavior, except for specific configurations such as $b'=2$ m and $H=60$ m, where variations in stress distribution occur. It is worth noting that an increase in the maximum water storage, H , affects the normal stress values, especially for values of X ranging from 10 m to 25 m. This indicates that there is a notable influence of water load on the stress distribution within this specific range, highlighting the complex interplay between dam section geometry, additional section length, and water storage capacity. These results emphasize the need for further analysis to comprehensively understand stress behavior and its implications for the design and performance of concrete dams.

Now, let us delve into the effects of H and b' on the normal stress of a concrete dam without a gallery, based on the results table provided. The table shows results for different values of H (60, 70, 80) at different distances, revealing a noticeable trend: as H increases, there is a corresponding increase in negative normal stress (P_v) values. This indicates that a higher dam height contributes to greater compressive forces on the dam structure over different distances. For example, at -1.49618 m, increasing H from 60 to 80 results in a more negative P_v , indicating increased compressive strength. Examining the effect of b' on normal stress, the results showed that as b' increased from 0 to 6, the P_v values tended to become less negative, indicating a decrease in the compressive forces on the dam. This is evident, for example, at distance -1.49618 m and H equals 60, where increasing b' from 0 to 6 results in a shift from a very negative P_v to a less negative one.

Analyzing both factors together, it becomes clear that increasing the height (H) leads to an intensification of compressive forces while increasing the width of the base b' has a mitigating effect. The interaction of these factors greatly affects the total normal pressure on a concrete dam without a porch. In summary, the height of the dam (H) and the width of the base (b') are important factors that

engineers must carefully consider to ensure the structural integrity and stability of the dam under different loading conditions.

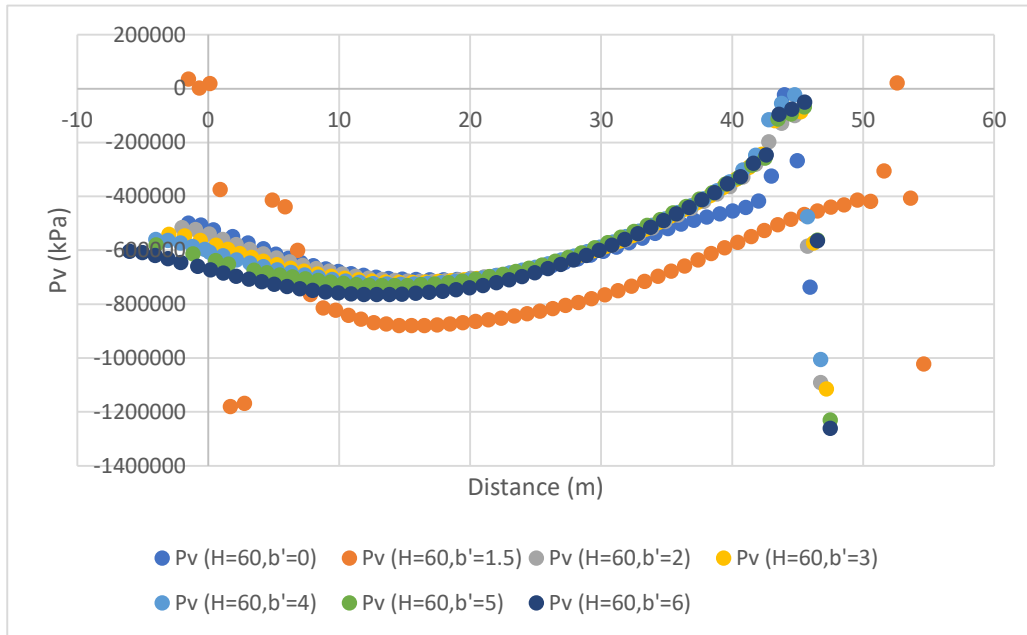


Figure 4: Variation of vertical stresses without gallery for $H=60$ m and different b' .

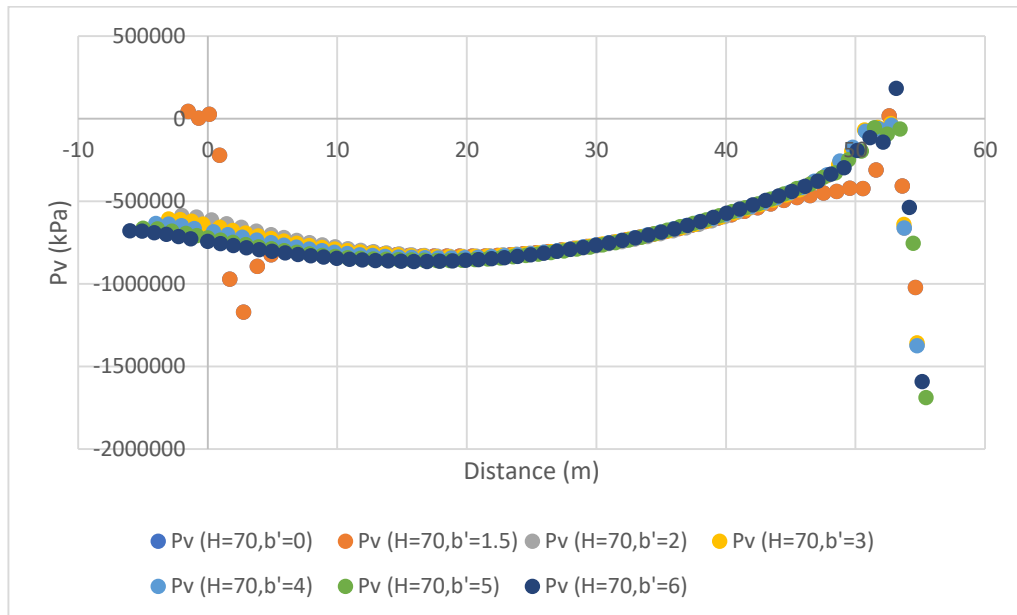


Figure 5: Variation of vertical stresses without gallery for $H=70$ m and different b' .

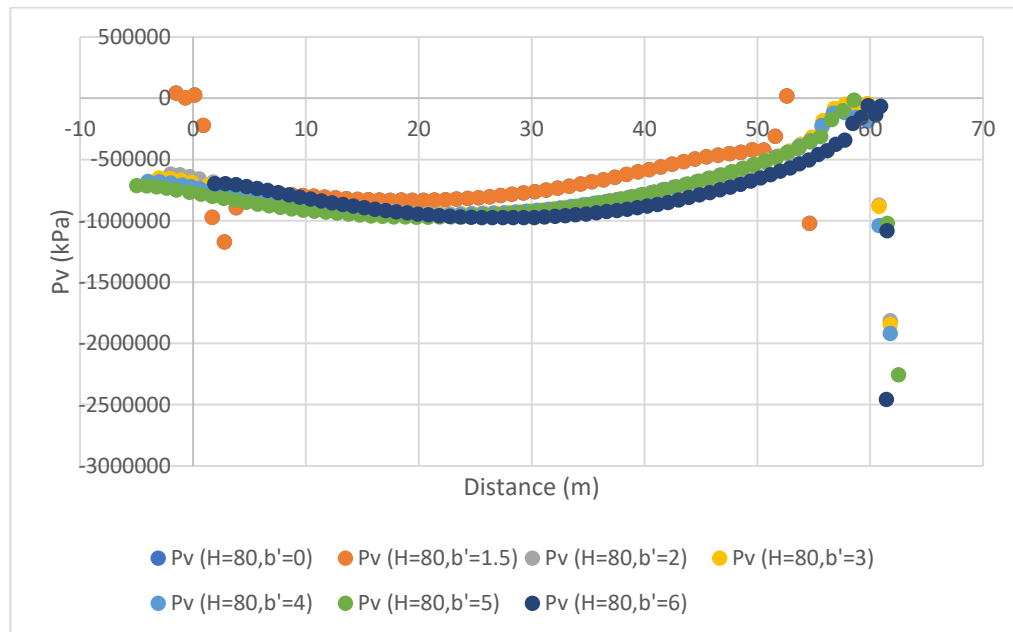


Figure 6: Variation of vertical stresses without gallery for $H=80$ m and different b' .

3.3 Principal Stress, σ , (with Gallery)

Examining the vertical stresses along the base of the concrete dam, taking into account variations in the maximum storage level (H) and the length of the additional core section (b'), provides valuable insights into the distribution and magnitude of principal stresses, as shown in Figures 7, 8, and 9. The presence of a gallery in a concrete dam greatly affects the stress distribution, in particular reducing the stress values within its perimeter and the surrounding area. Moreover, an increase in storage level corresponds to higher principal stress values, especially within the distance confined between 10 and 25 m. This relationship is due to the increase in hydrostatic pressure on the dam with increasing storage level, which confirms the interconnected nature of the factors affecting stress behavior in concrete dams. Consideration of gallery and storage level effects is critical to the design, analysis, and maintenance of concrete dams, ensuring structural integrity and performance under diverse loading conditions.

Further investigation of the effects of H (distance from the axis of the dam to the center of the gallery) and b' (width of the gallery) on principal stress reveals interesting patterns. Analysis of principal stress values for different distances along the dam axis with a constant gallery width (b' of 0) reveals consistency, implying a minimal effect on principal stress when changing H with constant b' . However, with increasing H , a noticeable trend of decreasing principal stress is observed, which is attributed to the increasing distance from the dam axis.

Shifting the focus to cases with constant H (e.g., $H = 60$) and varying gallery width b' , an increase in b' from 0 to 6 corresponds to a decrease in principal stress. This suggests that a wider gallery leads to lower principal stress, perhaps due to force redistribution or increased structural support.

Considering both H and b' together, variations in gallery width (b') exert a more pronounced influence on the principal stress than variations in distance from the dam axis (H). In cases where H is constant, an increase in b' continually results in a decrease in the principal pressure. However, observed anomalies in the data, where principal stress increases with increasing distance or gallery width, highlight the complexity of the relationship, necessitating further investigation in specific structural or geological conditions.

The results indicate that both the distance from the dam axis (H) and the gallery width (b') affect the principal stress of the concrete dam. The complex interaction between these variables emphasizes the need for comprehensive analysis to understand the specific relationships and optimize the design for stability and integrity under different loading conditions. Bottom of Form

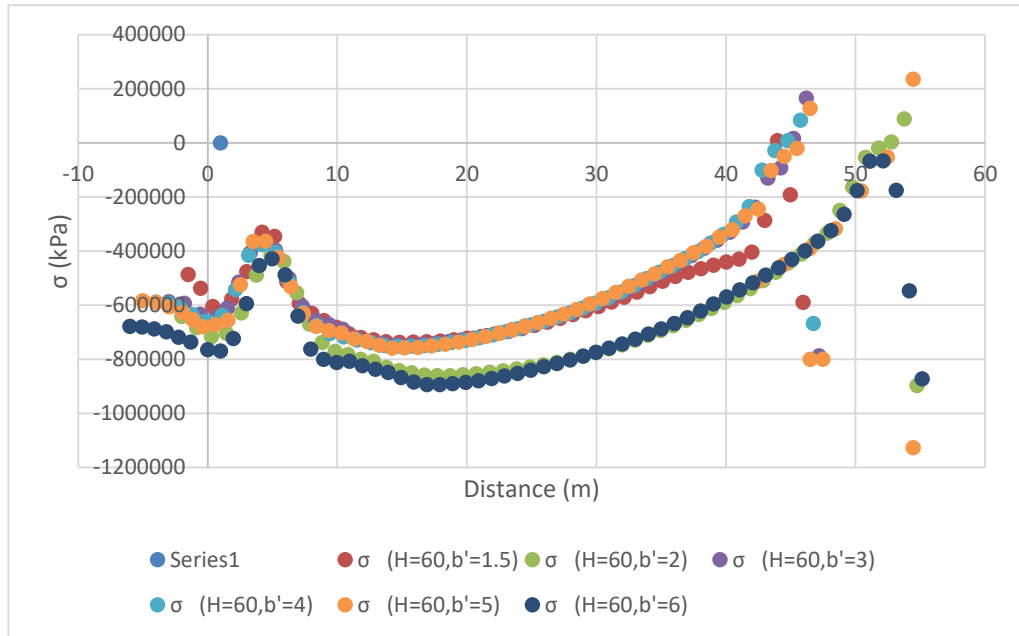


Figure 7: Variation of Principal stresses with gallery for H=60 m and different b'.

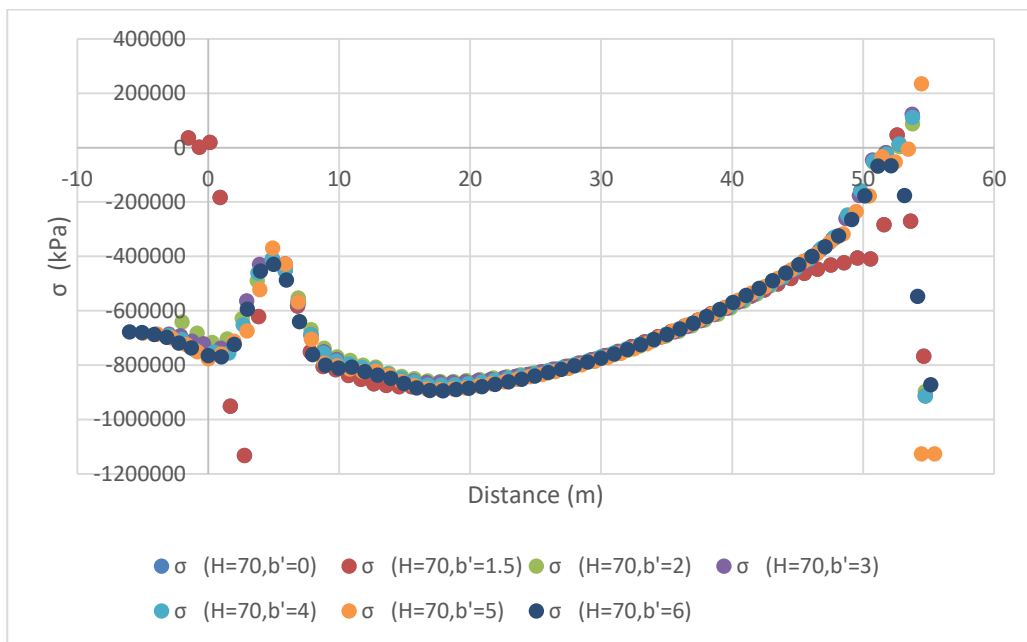


Figure 8: Variation of Principal stresses with gallery for H=70 m and different b'.

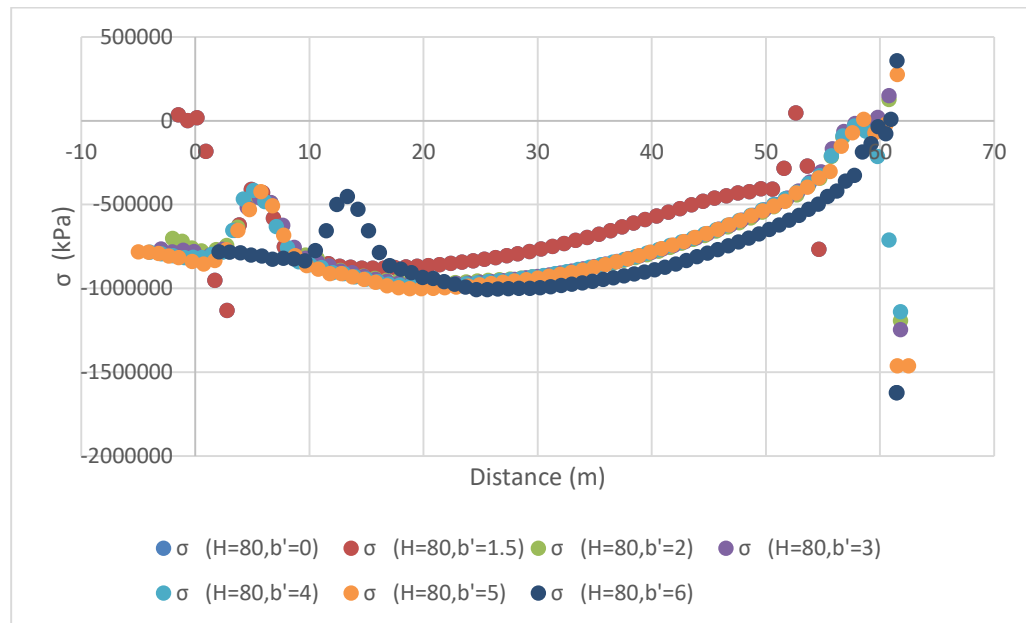


Figure 9: Variation of Principal stresses with gallery for $H=80$ m and different b' .

3.4 Principal Stress, σ , (without Gallery)

Figures 10, 11, and 12 provide valuable insights into the distribution of principal stresses along the base of the concrete dam in the absence of a gallery. In this scenario, the principal stresses show a distinct pattern characterized by a relative increase from the heel area up to a distance of 15 m along the base of the dam. After this point, pressure values gradually decrease until they reach the pre-toe area. It is worth noting that the drop in tension is not continuous but occurs over a specific distance. At the pre-toe-off point, a sudden increase in stress values is observed, indicating a localized stress concentration near this sub-exposure region.

The figures also state that the effect of the length of the additional section (b) on the principal stress values is quite limited, indicating the differences in their influence on the total stress distribution along the base of the concrete dam. However, this behavior may depend on the range of considered values of b and the characteristics of the dam structure. On the other hand, the number of increasing water levels H has a more pronounced effect on the principal stress values. As H increases, there is an increase in significant compensation, including conformity with expectations due to higher hydrostatic pressure.

Analyzing the results in terms of the effects of H (water height) and b' (distance from the dam axis to heel) on principal pressure without gallery provides further insights. As the dam height H increases from 60 to 80, the principal stress tends to decrease, indicating that higher dam structures exhibit lower stress levels, likely due to increased structural stability and distribution of loads over a larger area. In addition, examination of the effect of the distance from the dam axis to the gallery b' reveals that for a constant dam height, an increase in b' generally results in a higher principal stress, indicating that gallery location significantly affects stress distribution and may cause concentrations of Local stress. By focusing on a certain dam height, such as $H=70$, the principal pressure rises continuously with increasing b' , in line with the general trend. However, the rate of increase appears to decrease at higher values of b' , which may indicate a saturation effect where the effect of exposure to stress diminishes after a certain distance. The effect of b' is more pronounced at lower dam heights, such as $H=60$, confirming that the effect of gallery position is more important when the dam is relatively shorter.

In summary, the results confirm the complex relationship between dam height, gallery position, and principal stress. Higher dam structures generally show lower stress levels, while the distance from the dam axis to the gallery plays a crucial role in determining stress concentrations. The specific interaction between H and b' indicates a complex interaction between factors affecting the structural behavior of a concrete dam without a colonnade.

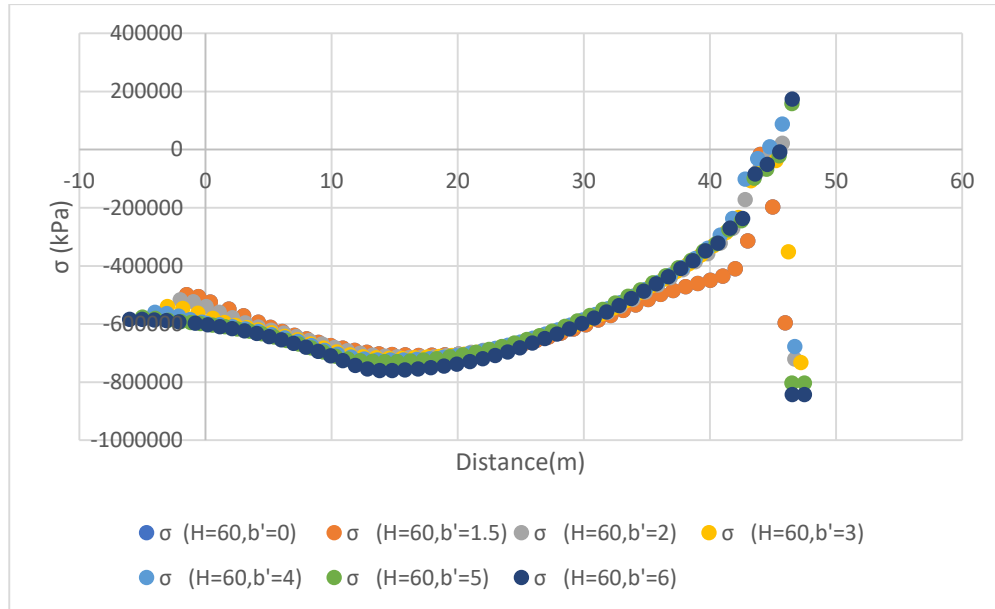


Figure 10: Variation of Principal stresses without gallery for H=60 m and different b'.

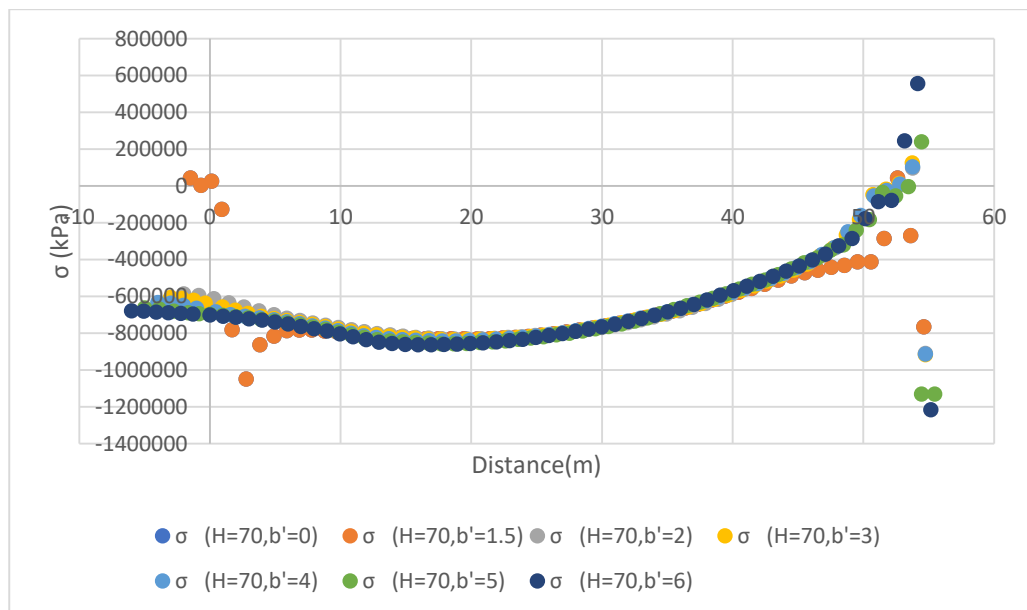


Figure 11: Variation of Principal stresses without gallery for H=70 m and different b'.

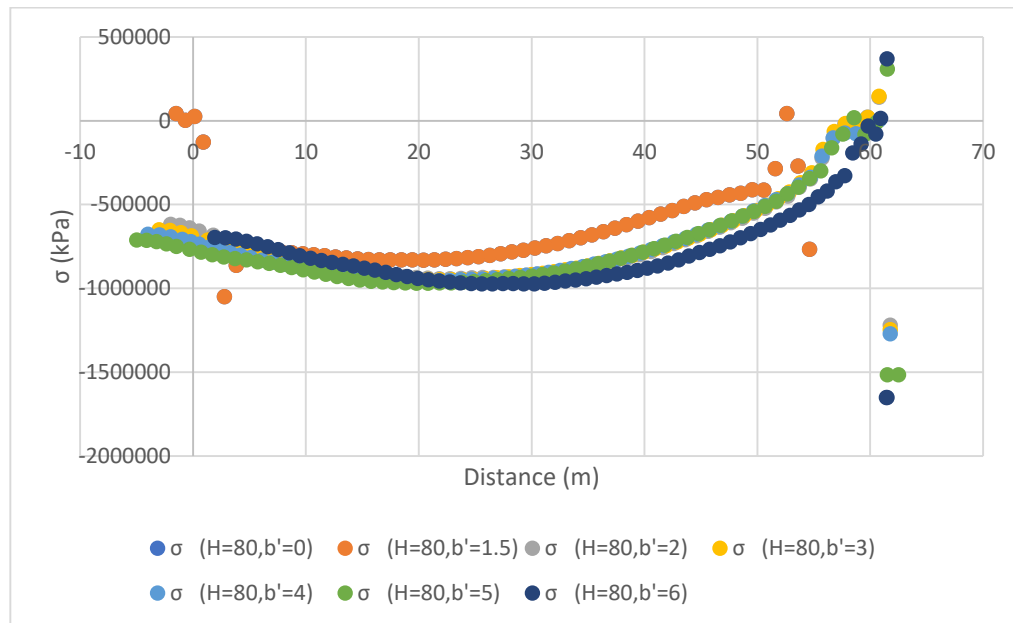


Figure 12: Variation of Principal stresses without gallery for $H=80$ m and different b' .

3.5 Shear Stress, τ , (with Gallery)

Examination of shear stresses on the concrete dam footing, taking into account the maximum stocking level (H) and the additional core length (b') in the presence of a gallery, are shown in Figures 13, 14, and 15. These figures provide valuable insights into the observed results, especially within the heel area. Embankment extending up to $X = 25$ meters. Here, there is no significant effect on the shear stress values for different combinations of H and b' . However, a noticeable change was observed at $X=5$ m due to the presence of the gallery. Moving beyond. In particular, when $H = 60$ and $b' = 6$ m, the shear stress values remain relatively constant, uniformly distributed toward the toe point of the weir. An increase in b' beyond 1.5 m results in higher shear stress values near the toe point of the dam, confirming the significant influence of additional core length (b') on shear stress values in this region. The effect of the maximum storage level (H) appears to have less influence on these values.

Analysis of the effects of H (weir height) and b' (weir base width) on shear stress provides additional insights. As the height of the dam (H) increases, the shear stress tends to decrease and is observed at the same distance for different H values. For example, at distance $D=43.9881$ m, the shear stress decreases from -4.21×10^6 ($H=60$, $b'=0$) to -6.00×10^6 ($H=80$, $b'=6$). This decrease is expected to occur due to additional hydrostatic pressure on the base of the dam. On the other hand, increasing the width of the dam base (b') generally leads to an increase in shear stress, which appears at the distance $D = 23.2028$ m.

The interaction between H and b' is complex and depends on specific sets of values. In general, as both H and b' increase, the shear stress tends to decrease, especially noticeable over larger distances (e.g., $D = 55.4505$ m). Other observations include shear stress varying with distance, negative values indicating compressive forces, positive values indicating tensile forces, and severe negative shear stress values indicating potential failure or instability of the dam structure.

In summary, the analysis highlights the important roles that the height and width of the dam base play in influencing shear stress. Higher embankments and narrower bases generally result in lower shear stresses, while wider bases tend to increase shear stresses. The specific interaction between these parameters requires careful consideration of the design and stability of the concrete dam.

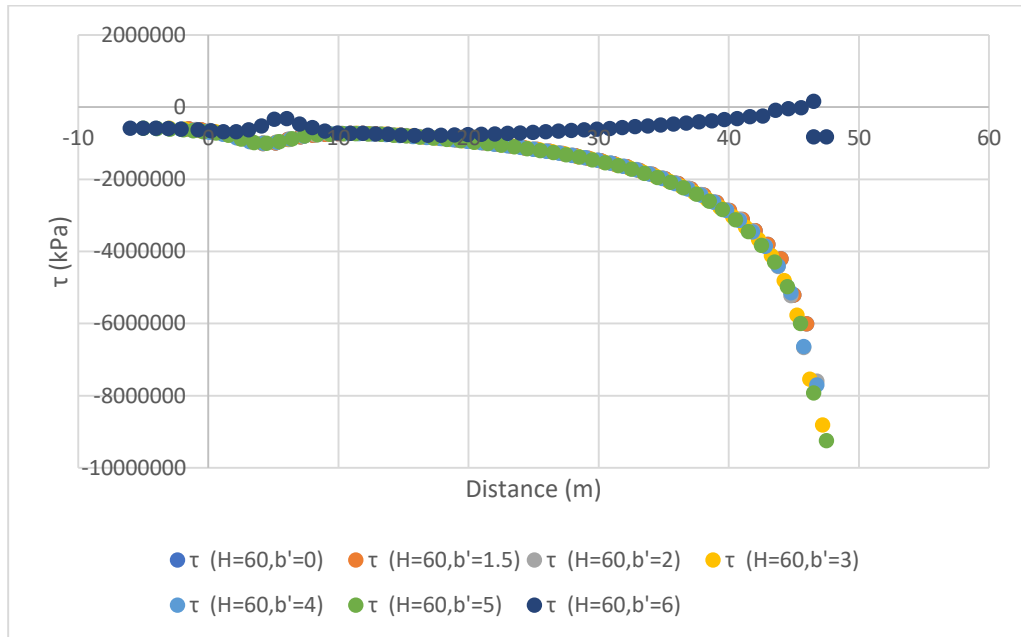


Figure 13: Variation of Shear stresses with gallery for $H=60$ m and different b' .

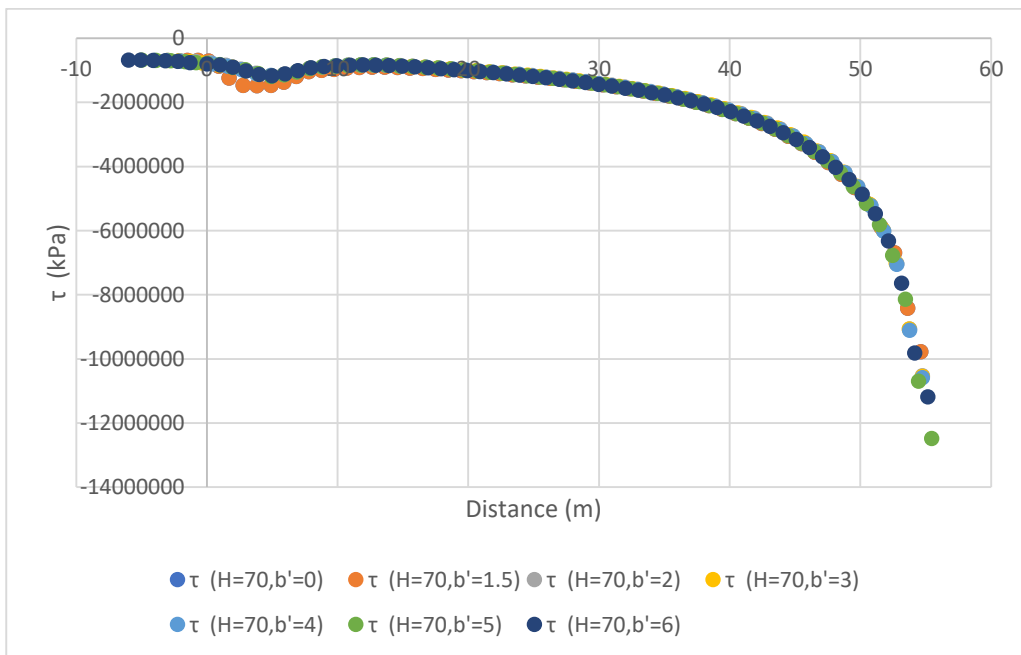


Figure 14: Variation of Shear stresses with gallery for $H=70$ m and different b' .

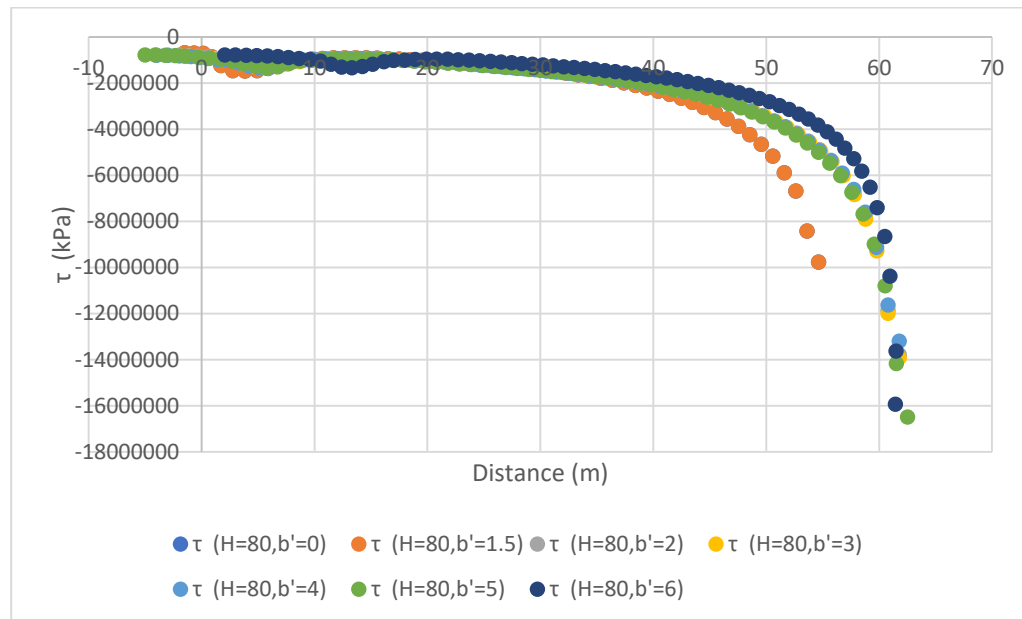


Figure 15: Variation of Shear stresses with gallery for $H=80$ m and different b' .

3.6 Shear Stress, τ , (without Gallery)

To comprehensively understand the effect of the maximum storage level (H) and the additional core length (b') of the concrete dam on the shear stresses, an investigation was performed in the absence of a gallery, as detailed in Figures 16, 17, and 18. The results provide valuable insights into the behavior and values of the stresses Shear along the base of the dam, taking into account different values of H and b' . While the observed pattern and values are very similar to those obtained in the previous case with a gallery, a noticeable difference arises due to the absence of any fluctuation in the shear stress values, especially near the upstream (U/S) side of the dam. The absence of the gallery results in a more uniform and consistent distribution of shear stresses along the base, emphasizing the influential role of the gallery in influencing shear stress values and introducing local dislocations or dislocations. These results underscore the importance of considering stress mitigation measures, such as gallery, in alleviating stress concentrations and ensuring the stability and integrity of the dam structure.

These results highlight the importance of considering changes in water level and the limited effect of additional section length when evaluating principal stress values in concrete dams. Proper analysis of these factors enables engineers to make informed decisions regarding the design, safety, and performance of concrete dams under various loading conditions. Understanding stress distribution patterns is crucial to the design and analysis of concrete dams. The observed stress behavior underscores the importance of incorporating a gallery or similar stress relief measures to mitigate stress concentrations and ensure the overall stability and integrity of the dam structure. Further analysis, taking into account other factors such as material properties, loading conditions, and dam geometry, would provide a more comprehensive understanding of stress distribution and facilitate more accurate design and safety assessments of concrete dams.

The results table displays the values of shear stress (τ) at different distances for different sets of parameters H (height) and b' (width) in the concrete dam. Analysis of the effects of H and b' on shear stress reveals distinct patterns for different height values. For $H = 60$ and varying values of b' (from 0 to 6), the shear stress tends to decrease with distance, with larger values of b' leading to lower shear stresses over the same distances. Similar trends are observed for $H = 70$ and $H = 80$, where increasing H generally leads to higher shear stress values over the corresponding distances. In addition, higher

values of b' still lead to lower shear stress, which confirms the importance of both height and width in influencing the shear stress in a concrete dam.

In summary, the analysis indicates that both H and b' play critical roles in determining shear stress in concrete dams. As the height of the dam increases, the shear stress tends to increase over the corresponding distances, while an increase in the width of the dam generally leads to a decrease in shear stress. The complex interplay between these parameters highlights the importance of a comprehensive understanding when evaluating shear stress distribution for effective design and safety considerations in concrete dams.

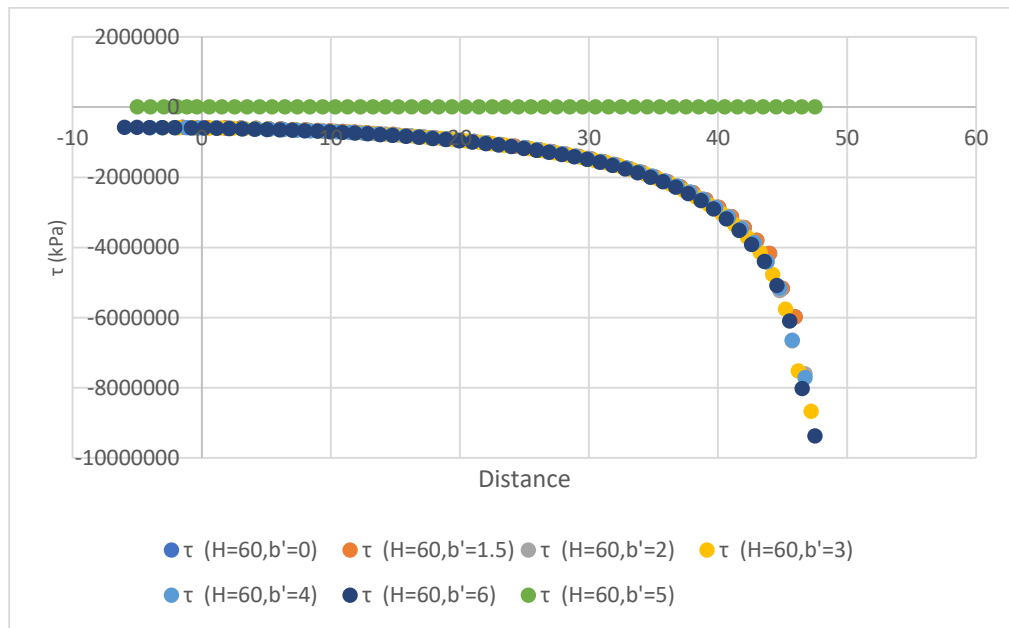


Figure 16: Variation of Shear stresses without gallery for $H=60$ m and different b' .

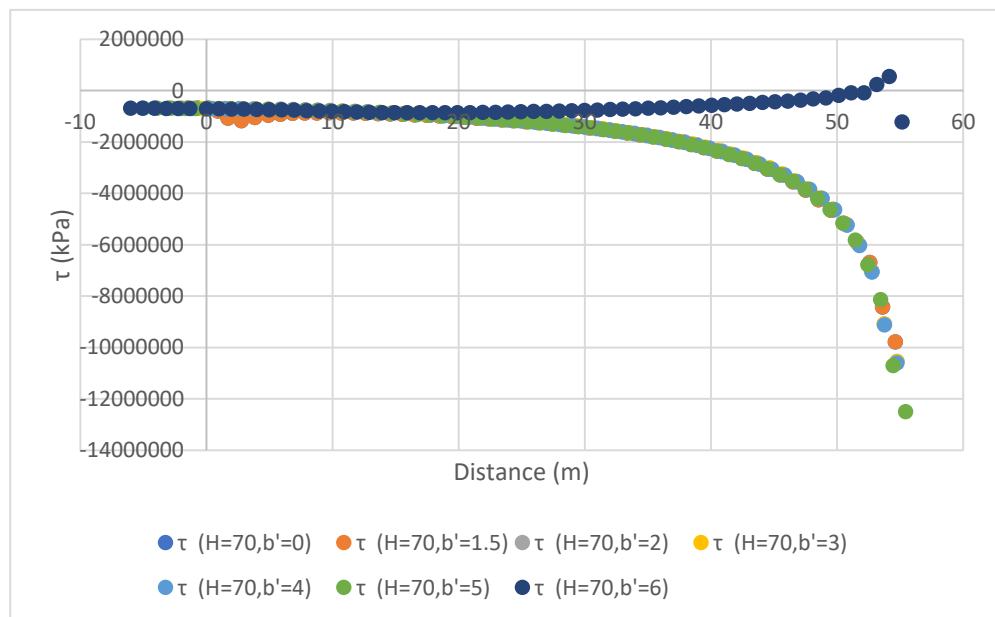


Figure 17: Variation of Shear stresses without gallery for $H=70$ m and different b' .

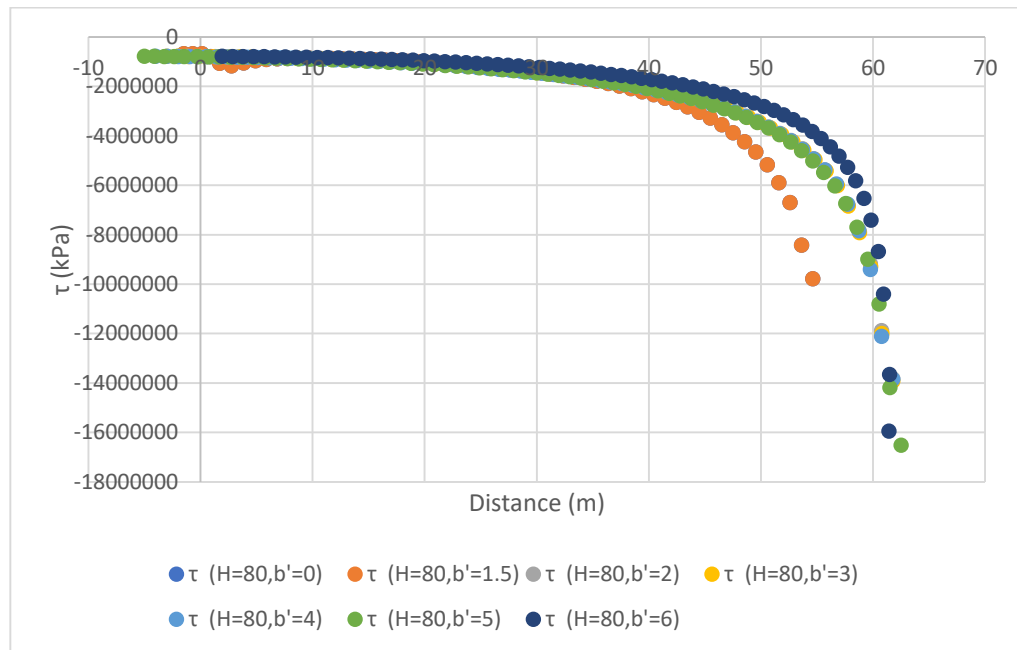


Figure 18: Variation of Shear stresses without gallery for $H=80$ m and different b' .

4. Conclusions

1. Exposure fronts create stress concentrations, affecting the distribution of pressure from the heel to the midsection. Increased water storage (H) raises the normal pressure slightly, while a wider base width reduces it, especially at higher elevations.
2. Without a gallery, the normal stress follows a characteristic shape from the heel to $X = 20$ m, decreases to $X = 45$ m, and peaks at the toe. The additional section length and increased water storage (H) affect the pressure within $X = 10$ m to 25 m.
3. Without a gallery, a higher embankment height (H) increases the negative normal stress (P_v), indicating greater compressive forces. Wider bases (b') reduce compressive forces. A high H intensifies compressive forces, while a high b reduces them. Gallery presence significantly reduces stress around and within the gallery. Increased storage (H) correlates with higher principal stresses, especially between 10 and 25 m.
4. The effects of H and b' on the principal stress show little effect on the constant b' while increasing H reduces the principal stress. Wider galleries contribute to less key pressure.
5. Combined H and b variations highlight the effect of gallery width on principal stress, with anomalies indicating complexity. Both H and b' affect the principal stress of the concrete dam.
6. The principal stress increases along the concrete dam base without a gallery up to 15 m heel, followed by a gradual decrease. There is a sudden increase in tension in the pre-toe area.
7. The additional section length (b) slightly affects the principal stress. Increasing the water level (H) results in increased principal pressures due to higher hydrostatic pressure. Analysis of H and b' effects on principal stress without a gallery reveals lower stress levels in higher dams with increasing H , indicating improved stability. Increased b' for a constant H results in higher principal stress.
8. . Focusing on specific water heights, such as $H=70$, shows a continuous rise in principal stress with increasing b' , consistent with the general trend. However, the rate of increase decreases at higher b' values, indicating the presence of a saturation effect. The effect of b' is more pronounced at low embankment heights (e.g., $H=60$).
9. Investigation of shear stresses on the foundation of a concrete dam reveals important results.

Within the heel zone of the dam up to $X = 25$ m, there is no significant effect on the shear stress values for different H and b' combinations. However, at $X = 5$ m, the gallery presents a noticeable change. An increase in b' of more than 1.5 m results in higher shear stress near the toe.

10. Further analysis of the effects of H and b' on shear stress highlights important trends. An increase in the dam height (H) is associated with a decrease in shear stress, which is attributed to the additional hydrostatic pressure. Widening of the dam base (b') generally results in increased shear stress.

Understanding the effect of H and b' on shear stresses in a concrete dam without a row of pillars results in a more uniform shear stress distribution along the base of the dam. The absence of the exhibition confirms its influential role in causing local unrest. The study emphasizes the importance of stress relief measures for stability and integrity, highlighting the limited impact of additional section length when evaluating major stress values. Incorporating an exhibition or similar stress-relieving measures is crucial.

5. Conflict of Interest

There is no conflict of interest in this paper

6. Acknowledgment

The researchers would like to thank Teşik International University for supporting scientific research efforts

7. Author's Contribution

"We confirm that the manuscript has been read and approved by all named authors. We also confirm that each author has the same contribution to the paper. We further confirm that the order of authors listed in the manuscript has been approved by all authors."

References

- [1] Ahmed TM. Effects of increasing the base on concrete dam stability. Eurasian J Sci Eng. 2016; 2(1): 10-20.
- [2] Corns CF, Tarbox GS, Schrader EK. Gravity dam design and analysis. In: Advanced dam engineering for design, construction, and rehabilitation. Boston, MA: Springer US; 1988. p. 466-492.
- [3] Das R, Cleary PW. A mesh-free approach for fracture modeling of gravity dams under earthquake. Int J Fracture. 2013;179(1):9-33. <https://doi.org/10.1007/s10704-012-9766-3>
- [4] Ghobarah A, Ghaemian M. Experimental study of small-scale dam models. J Eng Mech. 1998;124(11):1241-1248. [https://doi.org/10.1061/\(ASCE\)0733-9399](https://doi.org/10.1061/(ASCE)0733-9399)
- [5] Hamdi EJ, Al-Shadeedi MB. Stability evaluation of small concrete gravity dams. J Eng Sustain Dev. 2017;21(5).
- [6] Reclamation B. Design of gravity dams. A Water Resour Tech Publ, United States Dept Interior, Denver, Colorado. 1976.
- [7] Segura RL, Miquel B, Paultre P, Padgett JE. Accounting for uncertainties in the safety assessment of concrete gravity dams: A probabilistic approach with sample optimization. Water. 2021;13(6):855. <https://doi.org/10.3390/w13060855>
- [8] Zhu K, Gu C, Qiu J, Li H. The analysis of the concrete gravity dam's foundation uplift pressure under the function of the typhoon. Math Probl Eng. 2016. <https://doi.org/10.1155/2016/2834192>
- [9] Banerjee A, Paul DK, Acharyya A. Optimization and safety evaluation of concrete gravity dam section. KSCE J Civ Eng. 2015; 19: 1612-1619. <https://doi.org/10.1007/s12205-015-0139-0>

-
- [10] Folsom, Blue Stone. The investigation of effective parameters on the stability of concrete gravity dams with a case study. Am J Civ Eng Arch. 2014;2(5):167-173.
<https://doi.org/10.12691/ajcea-2-5-3>
-